
Structural Analysis of Gold Mineralization in the Southern Eureka Mining District, Eureka County, Nevada: A Predictive Structural Setting for Carlin-type Mineralization

Russell V. Di Fiori*, Sean P. Long, and John L. Muntean

Nevada Bureau of Mines and Geology, University of Nevada, Reno, NV, 89557, USA

Gary P. Edmondo

Timberline Resources Corporation, Coeur D'Alene, ID, 83814, USA

ABSTRACT

Identification of favorable structural settings for Carlin-type gold deposits is fundamental for future exploration. In this study, mapping and structural analysis were performed in the southern part of the Eureka mining district in east-central Nevada, in order to understand geometric and temporal relationships between structural systems and Carlin-type mineralization. 1:6,000-scale geologic and alteration maps of a ~3.5 km (east-west) by ~8 km (north-south) region were generated, along with cross sections that illustrate pre- and post-extensional deformation geometry. This project bridges a gap between recent 1:24,000-scale mapping and < 1:500-scale mapping performed in an active exploration campaign.

The stratigraphy of the map area consists of ~4 km of Cambrian-Devonian carbonate and siliclastic rocks, which are unconformably overlain and intruded by Late Eocene silicic volcanic rocks. Four structural systems are identified, consisting of Early Cretaceous contractional structures and three separate sets of normal faults: 1) 1st-order, kilometer-scale offset, down-to-the-west normal faults, including the Lookout Mountain and Dugout Tunnel faults; 2) 2nd-order, 10s to 100s meter-scale offset, north-striking normal faults, including the Oswego fault and the Rocky Canyon and East Ratto Ridge fault systems; and 3) a set of 3rd-order, meter-scale offset, east-striking normal faults that cut jasperoid bodies of presumed late Eocene age. The 1st- and 2nd-order faults cut Late Cretaceous intrusions and an associated contact metamorphic aureole, are overlapped by a late Eocene, sub-volcanic unconformity, and are interpreted to be contemporary.

In addition to lithology and structure, specific types of hydrothermal alteration and mineralization were mapped, including silicification, decarbonatization, dolomitization, quartz/calcite-veining, argillization, and the introduction of sulfides and their limonite weathering products. Carlin-type replacement mineralization, primarily hosted within Cambrian carbonate rocks, occurs in a series of deposits in the southern part of the map area. The deposits are associated with decarbonatization, silicification and jasperoid formation, and argillization, and are constrained as late Eocene or older by the overlap and intrusion of dated volcanic rocks.

The map area contains a km-scale, faulted relay-ramp of 2nd-order faults that transfer slip between synthetic 1st-order faults. Within accommodation zones, wall-damage zones are predicted to provide hydrothermal fluid pathways and therefore localize mineralization. The footwall of the Lookout Mountain fault, which contains the majority of Carlin-type deposits identified in the map area, contains a set of antithetic, 2nd-order normal faults, which is interpreted as a wall-damage zone that was responsible for controlling fluid-flow that led to mineralization.

The southern Eureka mining district contains several favorable structural condi-

*E-mail: rstle11@gmail.com

tions for Carlin-type gold mineralization, including: 1) normal fault systems that predated or were contemporaneous with late Eocene gold mineralization; and 2) complex normal fault interactions in an accommodation zone, including zones of dense fault intersections, antithetic normal faults, and fault-damage zones. These structural conditions were fundamental for generating a network of open-system fluid pathways, which created an ideal structural architecture for Carlin-type mineralization, and can be used as predictive tools for exploration elsewhere.

Key Words: structural control, Eureka, Carlin-type, accommodation zone, gold mineralization, fault damage zone

INTRODUCTION

The Eureka mining district occupies the southern end of the Battle Mountain–Eureka trend of Carlin-type gold mineralization in east-central Nevada (Figure 1), and contains a series of gold deposits (Nolan, 1962). Numerous geologic investigations of Carlin-type deposits have determined that the geometries of gold ore bodies commonly trend parallel to structures such as folds and faults (Peters, 2004), implying that hydrothermal fluid flow was structurally controlled. The Eureka min-

ing district hosts several Carlin-type gold deposits that occur in zones of deformation that are spatially associated with hydrothermal dissolution and jasperoidal breccia zones. The purpose of this study is to document structural controls on mineralization within the southern part of an actively explored portion of the Eureka mining district. Recent advances in understanding the large-scale structural geometry and deformation history of the Eureka district (Long et al., 2014A; 2014B), and the results of a drilling campaign by Timberline Resources, Corporation (TRC), a junior gold company actively exploring the district

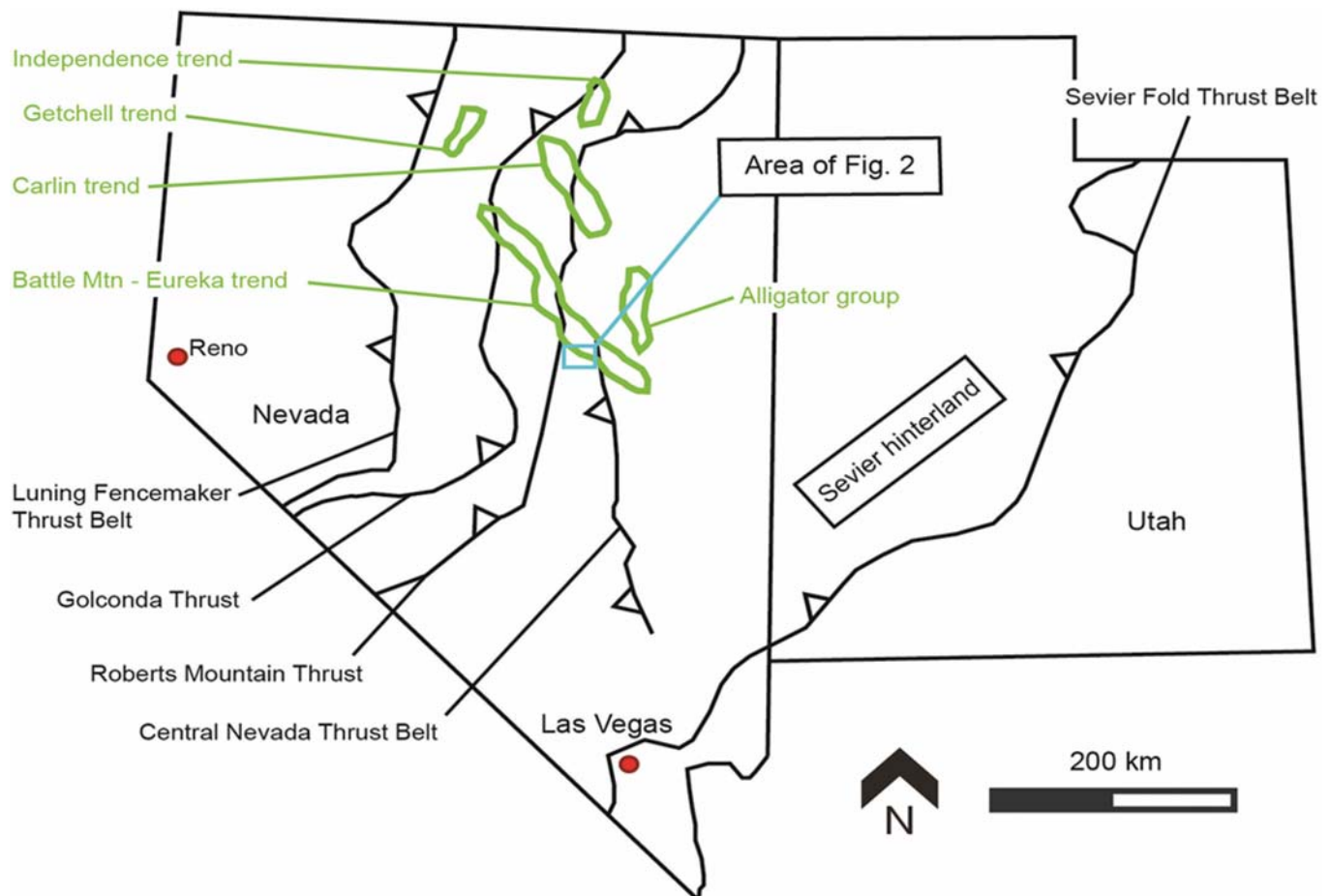


Figure 1. Location of study area relative to Paleozoic and Mesozoic contractional tectonic features. Blue box shows location of study area. Green polygons show location of major gold trends in northeastern Nevada. Modified from Long (2012) and Peters (2004).

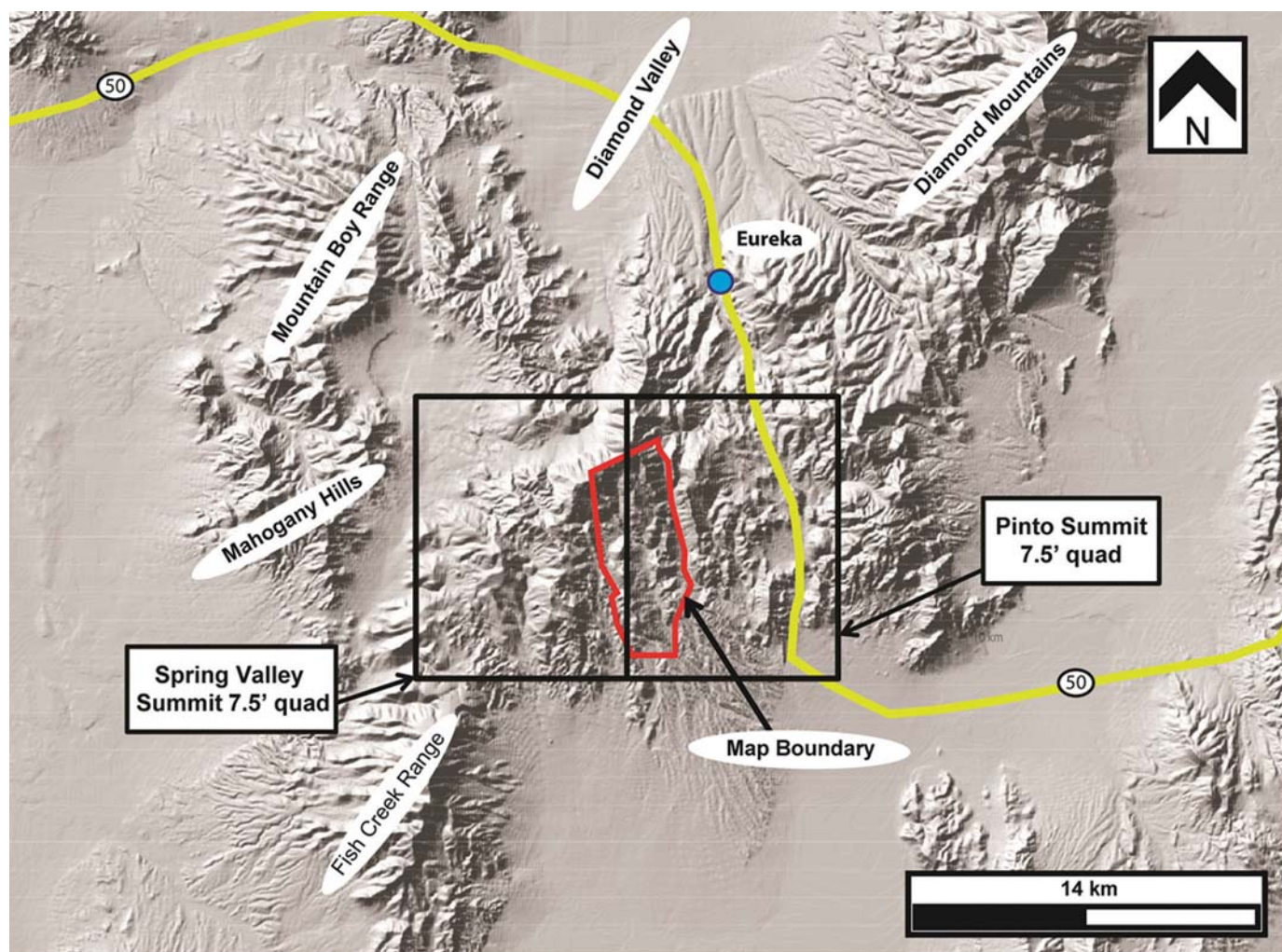


Figure 2. Map showing location of project area, with areas of adjoining USGS 7.5' quadrangles shown for reference. Red outline represents map boundary.

and a collaborator in this research, make a detailed evaluation of the relationships between structures, hydrothermal alteration, and gold mineralization both necessary and timely. Identifying structural controls on mineralization will assist in generating drill-hole targets for new deposits, and may lead to a better understanding of Carlin-type mineralization in general.

In this study, 1:6,000-scale geologic and alteration mapping of the region surrounding Lookout Mountain, an active TRC exploration site, was performed (Figure 2). The maps have been recently published at 1:10,000-scale (Di Fiori et al., 2014), and simplified versions are included here (Figure 9). In addition, geologic cross sections, supported by surface mapping data and TRC drill-hole data, were constructed (Figure 6A and 6B). As a second step, the cross sections were retro-deformed, with motions on extensional faults removed, in order to illustrate the pre-extensional deformation geometry. A gold grade-thickness map (Figure 8) was also constructed in order to gain insight into how fault systems may have influenced the distribution of mineralization. These data are utilized to generate a structural model, in order to help understand the temporal

and spatial evolution of alteration and mineralization, and to evaluate the degree to which structural architecture controlled hydrothermal fluid pathways.

Finally, this project tests a structurally framed model that accommodation zones between overlapping synthetic normal faults focus hydrothermal fluids and serve as controls on gold mineralization. Predictions for mineralization outboard of the primary faults within accommodation zones defined by Micklethwaite et al. (2010), Faulds and Heinz (2011), and Micklethwaite (2011) were tested by cataloging scaling relationships of structures within an accommodation zone, in conjunction with spatial patterns of alteration and gold mineralization.

GEOLOGIC SETTING

The Eureka mining district, and surrounding region of eastern Nevada, lies within the rifted western margin of the North American craton (Dickinson, 2002). During the early to mid-Paleozoic, the Eureka region was situated on the western edge of the continental shelf of the Cordilleran passive margin ba-

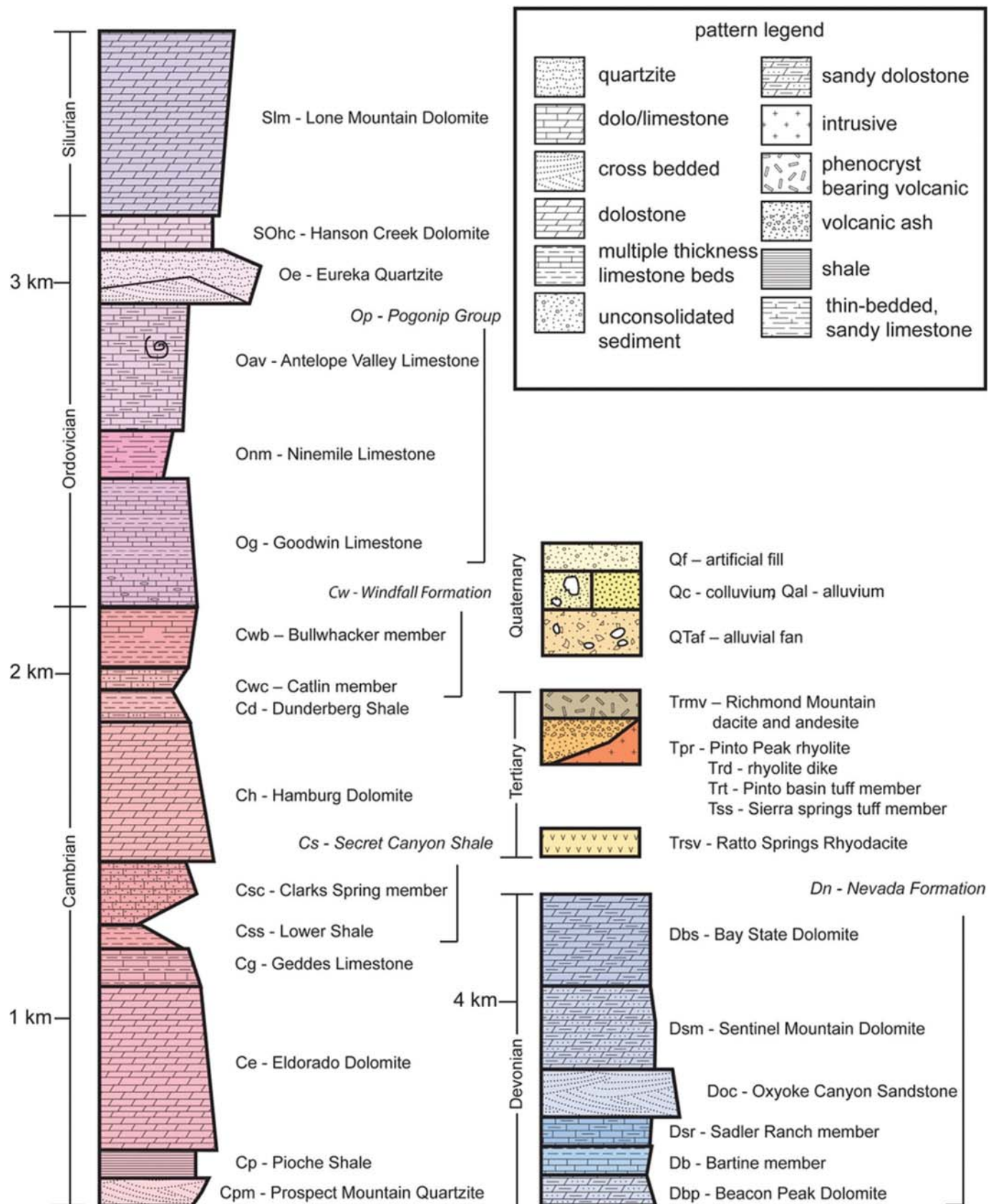


Figure 3. Stratigraphy of the map area.

sin, which was a vast carbonate platform (Stewart and Poole, 1974). The Cambrian to Devonian stratigraphic section consists primarily of limestone and dolostone interbedded with shale and sandstone (Figure 3) (Nolan et al., 1974). These carbonate rocks, particularly the Cambrian section, serve as the dominant host rocks for mineralization in the district.

During the Late Devonian and Early Mississippian, the Antler orogeny, a contractional deformation event involving east-vergent thrusting of deep-water sedimentary rocks of the Roberts Mountain allochthon over the western edge of the continental shelf, affected the region immediately west of the map area (Figure 1) (Speed and Sleep, 1982). The Eureka region occupied a foreland basin that subsided to the east of the allochthon, which was filled with clastic sediment shed from the eroding highlands to the west. This deposition is represented by a ~1.5 km-thick section of Mississippian conglomerate and shale (Nolan et al., 1974).

During the Jurassic-Cretaceous Cordilleran orogenic event, the Eureka mining district was situated between the Jurassic Luning-Fencemaker thrust belt in western Nevada (Oldow, 1984; Wyld, 2002) and the Cretaceous Sevier fold and thrust belt in Utah (Figure 1) (e.g., Armstrong, 1968; DeCelles and Coogan, 2006). Uplift and erosion during the Sevier orogeny is interpreted to be responsible for the erosion of any Mesozoic strata that would have been deposited prior to eruption of Eocene-Oligocene volcanic rocks (Long, 2012). The Eureka region is situated within the Central Nevada thrust belt (Taylor et al., 1993; Long, 2012), a system of north-striking contractional structures which can be bracketed between Permian and Late Cretaceous (Taylor et al., 2000), and in some places as Early Cretaceous (Long et al., 2014B). Long et al. (2014A) proposed that the large-scale structure of the Eureka mining district can be explained by Early Cretaceous growth of a regional-scale anticline, the Eureka culmination, associated with east-vergent motion on the blind Ratto Canyon thrust, which is defined by a Cambrian over Silurian relationship in drill holes beneath Lookout Mountain and Rocky Canyon, in the southern part of the map area (Figure 4).

Cretaceous contractional deformation was followed by extension accommodated by several large-throw (100s to 1000s of meters) normal faults, which are bracketed between Late Cretaceous and late Eocene (Long et al., 2014B). In the map area, the largest-offset (2,000–4,000 meters) normal faults are the Dugout Tunnel and Lookout Mountain faults (Di Fiori et al., 2014). These structures are superposed by multiple smaller-scale (10s to 100s of meters offset) normal faults, generally striking north to north-east.

Cenozoic magmatism began at ca. 45 Ma in northeastern Nevada, and was part of a southwestward-migrating belt of rhyolitic and andesitic magmatism called the Great Basin ignimbrite flare-up (e.g., Best et al., 2009). In northeastern Nevada this magmatism was dominated by andesitic and dacitic lavas and compositionally-similar intrusions (Henry, 2008). In the Eureka region, ignimbrite flare-up rocks included late Eo-

cene (~37–33 Ma) silicic ash falls and flows, tuffs, and intrusive volcanic rocks (Nolan et al., 1974; Long et al., 2014A).

More recently, Nevada has been the site of regional extension associated with formation of the Basin and Range extensional province, which is interpreted as the result of the extensional regime introduced by the establishment of the San Andreas transform fault system, the active plate boundary between the North American plate and the Pacific plate, beginning in the middle Miocene (e.g., Dickinson, 2002). The map area resides in the Fish Creek Range, and is surrounded by adjacent modern basins, mountains, and valleys, including the Diamond Mountains, Diamond Valley, the Mountain Boy Range and the Mahogany Hills (Figure 2).

METHODS

Geologic and alteration mapping

Geologic mapping of the Rocky Canyon, Oswego, and Lookout Mountain structural trends (Figure 5A) was conducted at a scale of 1:6,000, and is published along with five deformed cross sections at 1:10,000-scale (Di Fiori et al., 2014). A simplified version of the geologic map is shown in Figure 4. Field-based mapping was supplemented by interpretation of 1:24,000-scale aerial photography, and was completed on hand-drafted overlays draped over 1:6,000 scale orthoimagery and topography. Drafting of the overlays was completed in ArcMap 10.1 with annotations performed in Adobe Illustrator CS6. The map area is centered on TRC's Lookout Mountain exploration site (Figure 2). The location of the study area was chosen based on TRC's existing exploration effort, and the map boundaries were chosen based on the spatial extent of the Rocky Canyon, Lookout Mountain, and Oswego structural trends (Figure 5A), as well the locations of known occurrences of mineralization.

Mapping of hydrothermal alteration and mineralization was completed as an overlay over geologic data using methods developed by the Anaconda Mining Company (Brimhall, 2006). Specific types of hydrothermal alteration and mineralization products that were mapped include jasperoid (silicification of limestone), decarbonatization of carbonate host rock, argillization, and sulfides (mainly pyrite) and their limonitic weathering products. A simplified version of this alteration map is included here as Figure 9.

Cross sections

The published geologic map (Di Fiori et al., 2014) is accompanied by five 1:10,000-scale deformed geologic cross sections, which are constrained by map data, stratigraphic thicknesses, and the apparent dip of strata. In addition, the cross sections are constrained by drill-hole data from TRC's ongoing exploration and development campaign. The cross sections were drafted along transects perpendicular to the strike of major structures and the dominant regional strike of bedding (Figure

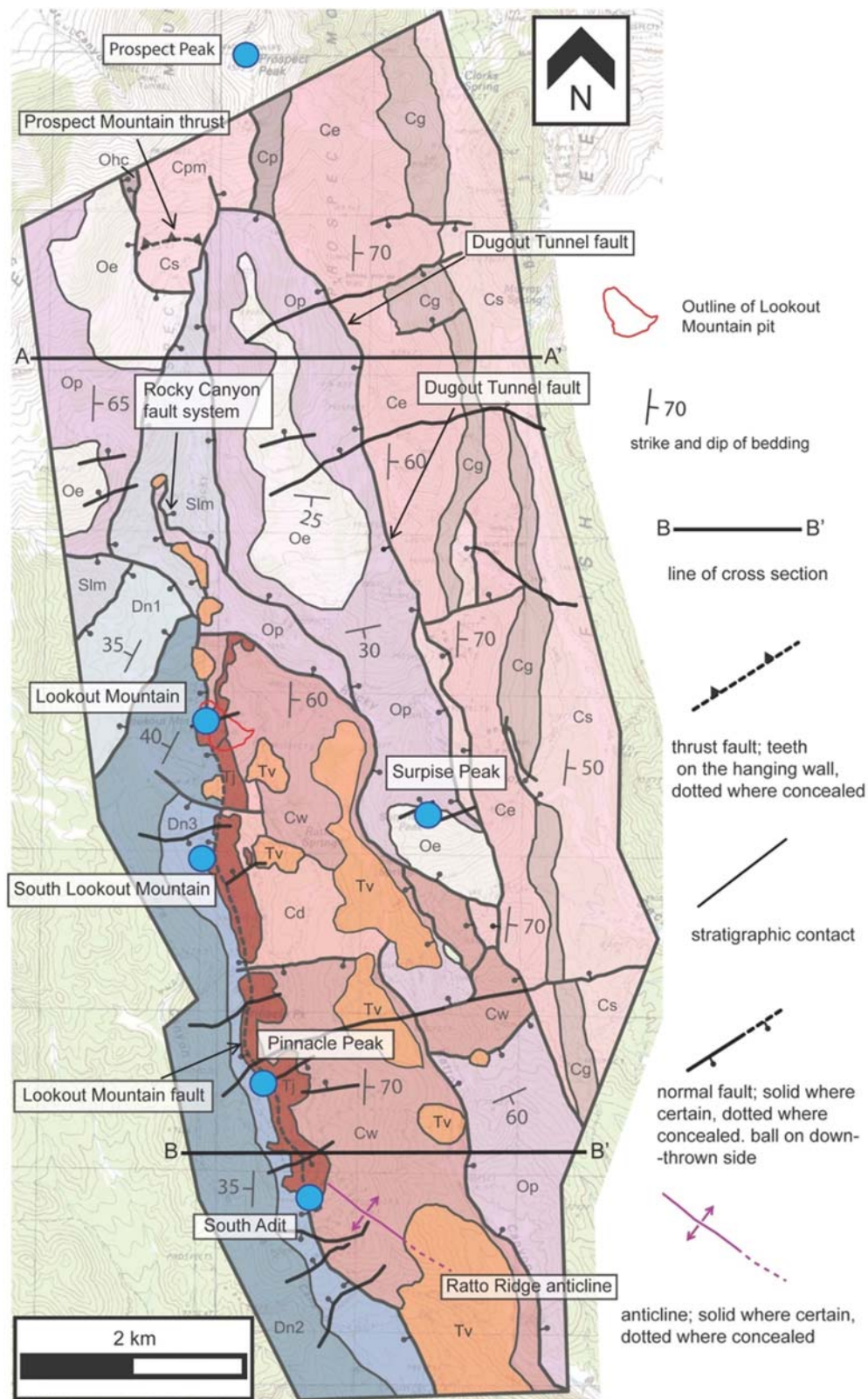


Figure 4. Geologic map of project area (simplified from Di Fiori et al., 2014). Refer to Figure 3 for guide to map units. Simplified Devonian map units include: Dn1 (Oxyoke Canyon Sandstone, and Bartine and Sadler Ranch members of Nevada Formation, undifferentiated), Dn2 (Oxyoke Canyon Sandstone and Sentinel Mountain Dolomite, undifferentiated), and Dn 3 (Bay State Dolomite). Unit Tv represents units Trsv, Tpr, and Trmv, undifferentiated. Quaternary units are omitted for simplicity.

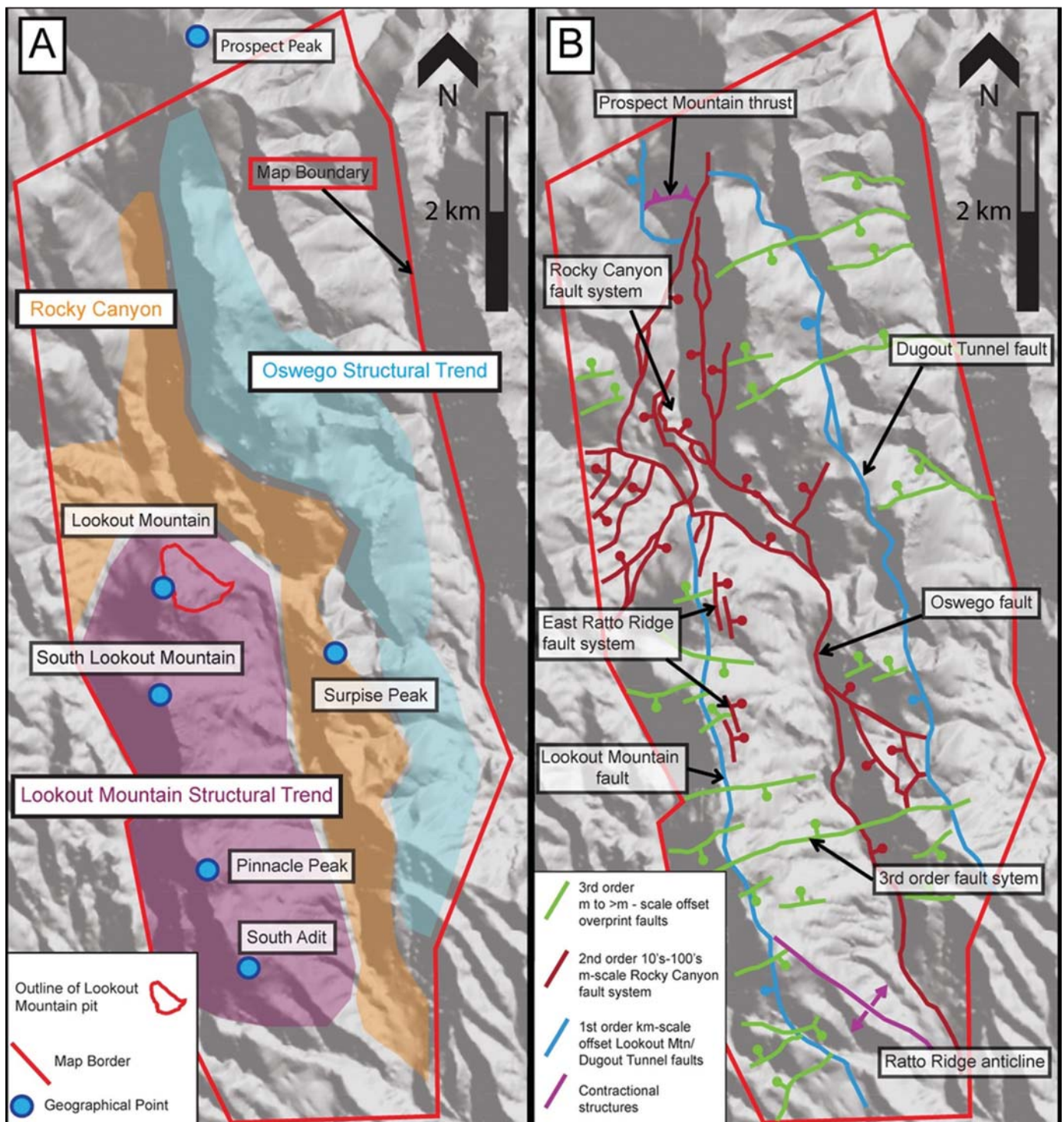


Figure 5. A) Structural trends of the map area, including the Lookout Mountain trend (purple), Rocky Canyon system (orange), and Oswego trend (blue). Geographic localities discussed in the text are also labeled, as well as the Lookout Mountain open pit outlined in pink. B). Simplified map of fault systems in the map area. Faults are classified by order, representing offset amount.

4). The original versions of the cross sections were drafted by hand, and Adobe Illustrator CS6 was used in drafting and annotating the final sections. Here, simplified versions of two of the five published cross sections are shown in Figure 6, along

with retro-deformed versions of each cross section that show pre-extensional geometry.

Regions of similar apparent dip on the cross sections were used to define dip domains. The boundaries between adjacent

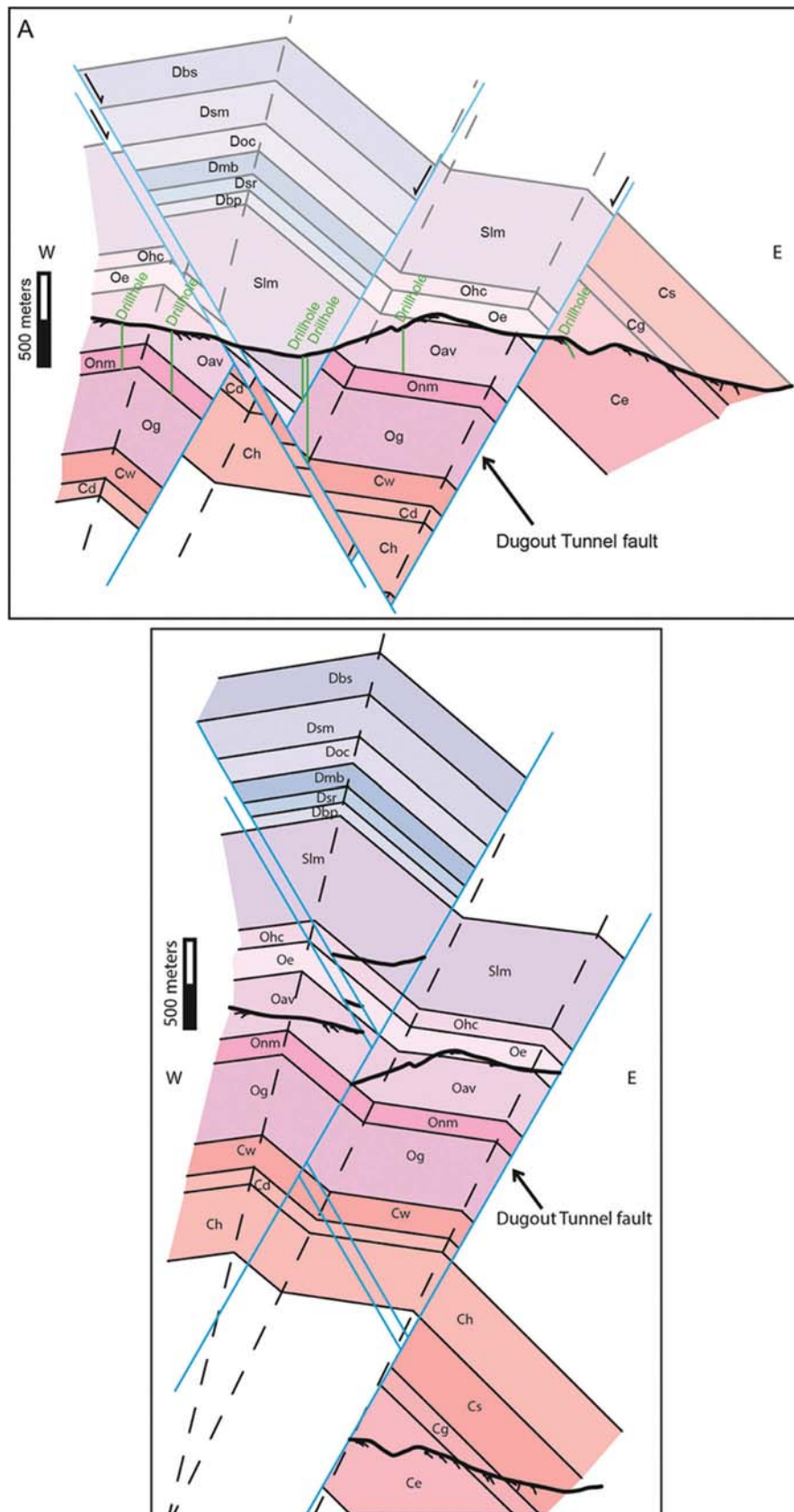


Figure 6A. Deformed and retro-deformed cross sections (simplified from Di Fiori et al., 2014): (A) North Rocky Canyon cross section (A-A' on Figure 4).

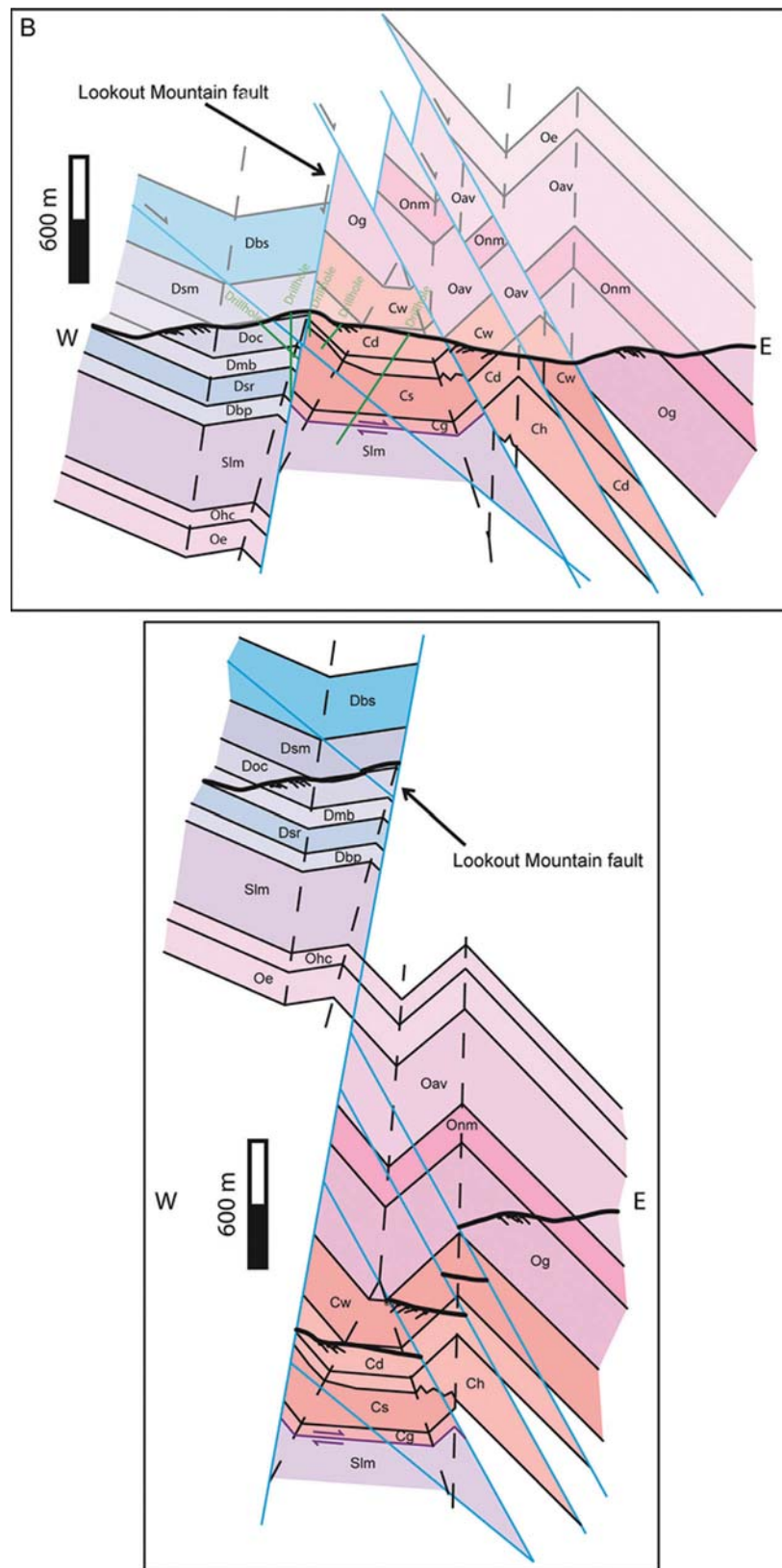


Figure 6B. Deformed and retro-deformed cross sections (simplified from Di Fiori et al., 2014): (B) South Adit cross section (B-B' on Figure 4). Blue lines are faults, thin black lines are stratigraphic contacts, and thick black lines are the modern erosion surface. Green lines represent TRC drill holes. Quaternary and Tertiary map units are omitted for simplicity.

dip domains were treated as kink surfaces (e.g., Suppe, 1983), and their orientation was determined by bisecting the intersection angle of the two domains. Dip domains, line lengths, angles, and fault offsets were matched between the deformed and restored cross sections (e.g., Dahlstrom, 1969). In addition, eroded stratigraphy above the modern erosion surface is drafted on the cross sections. The versions of the cross sections shown here omit overlying Quaternary units and Tertiary volcanic rocks for simplicity.

STRATIGRAPHY

The map area contains exposures of Paleozoic rocks ranging from Early Cambrian to Late Devonian, with a cumulative thickness of ~4.3 km, which are dominated by limestone and dolostone, with lesser quartzite and shale (Figure 3). Tertiary rocks in the map area include late Eocene volcanic rocks, including andesite, dacite, and rhyolite flows, and ash-flow tuffs, dated between ~36–37 Ma (Long et al., 2014A), as well as collapse breccia and jasperoid bodies interpreted to be contemporaneous with Carlin-type mineralization. Quaternary deposits in the map area include alluvium in modern stream drainages, hillslope colluvium, and alluvial fan systems. Detailed lithologic descriptions of all map units are included in the published map (Di Fiori et al., 2014); while lithologic descriptions are not included here, stratigraphic relationships and thicknesses are summarized on Figure 3.

STRUCTURAL FRAMEWORK

The project area contains four sets of structural systems. These include Early Cretaceous contractional structures and three separate sets of overprinting extensional systems: 1) 1st-order, km-scale offset, down-to-the-west normal faults, which include the Lookout Mountain fault and the Dugout Tunnel fault; 2) 2nd-order, 10s to 100s meter offset normal faults, including the Oswego fault, and the Rocky Canyon and East Ratto Ridge fault systems. Both the 1st- and 2nd-order fault sets can be bracketed between Late Cretaceous (~86 Ma), the age of the contact metamorphism halo that is cut by the Dugout Tunnel fault, and late Eocene (~37 Ma), the age of the oldest volcanic rocks that overlap these faults across an angular unconformity (Long et al., 2014B). Lastly, 3): a set of 3rd-order, meter-scale offset, east-striking normal faults cut jasperoid bodies of presumed late Eocene age.

Contractional structures

Thrust faults and folds within the map area record the earliest deformation, and form the structural architecture that was superposed by extensional faults. Map-scale contractional structures include the Prospect Mountain thrust, Ratto Canyon thrust, and Ratto Ridge anticline.

The Prospect Mountain thrust, an east-vergent, shallowly-

dipping thrust fault (Long et al., 2014B), is observed in the northern area of the map, in the northern end of Rocky Canyon (Figures 4 and 7). This fault places lower Cambrian Prospect Mountain Quartzite over Cambrian Secret Canyon Shale, which defines an older-over-younger relationship. This structure can also be traced to the north; it is exposed on the north side of Prospect Mountain, ~1 km north of the map area (Long et al., 2014A). Top-to-the-east offset on the Prospect Mountain thrust is estimated at ~850 m (Long et al., 2014B). The Prospect Mountain thrust is cut on the west by the Dugout Tunnel fault and cut on the east by a down-to-the-east normal fault.

The Ratto Canyon thrust (Long et al., 2014A; 2014B) is defined by drill-hole data on the east slope of Lookout Mountain, and does not breach the modern erosion surface within the map area. This blind thrust places Cambrian Secret Canyon Shale and Geddes Limestone over Silurian Lone Mountain Dolomite. This older-over-younger relationship is observed in two drill holes on the east flank of Lookout Mountain, as well as on Ratto Ridge at South Adit (Figure 6B). The Ratto Canyon thrust is only observable in drill core, and therefore little is known about its map-scale extent and geometry. Silurian Lone Mountain Dolomite and conodonts correlative in age to the Ordovician Hanson Creek Dolomite were obtained from rocks within the footwall of the thrust, which agrees with observations of drill core (Long et al., 2014B).

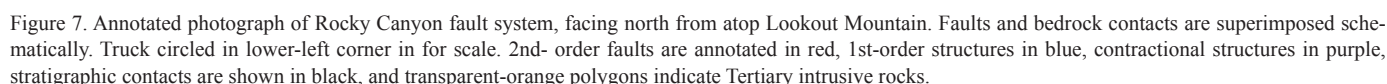
A north to north-northwest striking anticline axis can be traced near-parallel with the Lookout Mountain ridgeline (Figure 4 and 5B), and is here named the Ratto Ridge anticline. North of Pinnacle Peak, Devonian strata dip gently to the west (~20°) on the west side of the Lookout-Ratto Ridge ridgeline. On the eastern flank of the ridgeline, Cambrian strata typically dip moderately (~30–50°) to the east. Southeast of South Adit, a northwest-trending anticline axis is observed (Figure 4 and 5B), and is truncated by a jasperoid outcrop at the ridgeline. This is interpreted to be the southern extent of the axis of the Ratto Ridge anticline. The fold axis appears to have served as a plane of weakness that was later exploited by the Lookout Mountain normal fault. Down-to-the-west motion on this fault has dropped the fold axis of the anticline below the modern erosion surface in the hanging wall of the Lookout Mountain fault.

Extensional structures

Extensional structures within the map area vary in offset, ranging from meter-scale to a few kilometers.

First-Order Normal Faults

Lookout Mountain is bisected by a north-striking, steeply (~75–80°) west-dipping normal fault, the Lookout Mountain fault, which places Devonian strata on the west against steeply east-dipping Cambrian strata on the east (Figure 4 and 6A-B). The Lookout Mountain fault has ~2.3 kilometers of offset in the southern half of the map area (Figure 6B). North of Lookout Mountain, the fault disperses into the Rocky Canyon fault



The other 1st order normal fault in the map area is the north-striking, steeply ($\sim 60^\circ$) west-dipping Dugout Tunnel fault, which places shallowly east-dipping Ordovician rocks over steeply east-dipping Cambrian rocks along the full length of the map area (Figures 4 and 6). At the north end of the map area, the fault places Ordovician Hansen Creek Dolomite against Cambrian Prospect Mountain Quartzite, corresponding to ~ 3 km of offset. In northern Rocky Canyon, the strike changes to east-west, and the fault cuts nearly perpendicularly up section in its footwall from the Prospect Mountain Quartzite to the Eldorado Dolomite. In the adjacent canyon, the Dugout Tunnel fault regains its original north strike. The northern half of the Oswego trend is bisected by the Dugout Tunnel fault, which places Ordovician Eureka Quartzite and Antelope Valley Limestone on the west against Cambrian Eldorado Dolomite on the east. Subsidiary synthetic faults that branch off of the master fault place Secret Canyon Shale over Eldorado Dolomite. South of Sur-

Both the Lookout Mountain and the Dugout Tunnel faults are overlapped by the late Eocene (ca. 37 Ma) sub-volcanic unconformity, which provides a youngest permissible motion age (Long et al., 2014B).

The down-to-the-east Oswego fault strikes northwest through Rocky Canyon, and strikes north through Ratto Canyon. East of Lookout Mountain, the fault places Ordovician Antelope Valley Limestone over Cambrian Dunderberg Shale, corresponding to ~900 meters of offset. West of Surprise Peak, this structure bifurcates into two strands. One strand can be traced to the south, where the fault loses throw, is only exposed in short segments, and omits little strata, possibly removing parts of the sections of the Cambrian Windfall Formation or the overlying Ordovician Goodwin Formation. The second fault strand, just

to the south of Surprise Peak, strikes southeast where it merges with the Dugout Tunnel fault within a complex fault network (Figure 4 and 5B). This 2nd-order system can be bracketed as pre-Late Eocene, as it is overlapped by the sub-volcanic unconformity in Ratto Canyon.

Another important group of 2nd-order faults is the Rocky Canyon fault system (Figure 5B). On the north side of Lookout Mountain, throw on the Lookout Mountain fault decreases by ~900 meters within a north-south map distance of ~350 meters. To the north, some of this offset is accommodated by an array of faults that strike north and northwest into Rocky Canyon, here named the Rocky Canyon fault system (Figures 4 and 5B). At the south end of Rocky Canyon, a narrow, ~900 meter-long horst of Ordovician Pogonip Group rocks is observed, and is bound on the east and west by normal faults which down-drop Silurian rocks. On both flanks of Rocky Canyon, normal faults place Silurian Lone Mountain Dolomite against Ordovician Eureka Quartzite and Antelope Valley Limestone, defining Rocky Canyon as a complexly faulted graben. The horst of Ordovician rocks is interpreted to be the result of an older down-to-the-east fault being truncated and displaced by a younger down-to-the-west fault (Di Fiori et al., 2014). The faults bounding this horst cannot be mapped further to the north after their traces meet. However, the faults bounding the Rocky Canyon graben converge on one another in the northernmost part of Rocky Canyon. Here, either one fault terminates, or these two faults merge; cover by colluvium prevents analysis of their crosscutting relationship. The Dugout Tunnel fault is cut and offset by the northward continuation of this structure at the northern end of the map area (Figure 4 and 5B). Along the Rocky Canyon horst, several dikes, which are interpreted to be late Eocene in age due to similar characteristics of dated nearby intrusions, intrude along some of these faults, constraining this structural system to be pre-late Eocene (Figures 4 and 7).

Lastly, a set of east-dipping, north-striking faults with 10s to 100s m-scale offset, can be observed in the footwall of the Lookout Mountain fault, within 1 km of its trace, which are here grouped together as the East Ratto Ridge fault system. While these faults are not expressed at the surface due to extensive cover by colluvium, they are documented in drill-holes (Figure 8 A-B), where they attenuate the Cambrian Hamburg Dolomite and down-drop the Cambrian Dunderberg Shale and Windfall Formation. These faults are also overlapped by the sub-volcanic unconformity, indicating that they are also pre-late Eocene.

Third-Order Normal Faults

A series of irregularly spaced, east to northeast striking normal faults are distributed over much of the map area, and are exposed primarily in ridgeline outcrops within the Oswego and Lookout Mountain structural trends (Figure 5A and 5B). These faults typically exhibit meter- to sub-meter scale offset magnitudes. These faults cross-cut the 1st-order Lookout Mountain and Dugout Tunnel faults and associated jasperoid replacement bodies, and therefore are interpreted to be post-late Eocene.

Jasperoid replacement bodies and competent stratigraphic units including the Ordovician Eureka Quartzite and Cambrian Eldorado Dolomite preserve slickenlines that record predominantly dip-slip motion on these faults.

ALTERATION AND MINERALIZATION

Hydrothermal alteration and mineralization mapping

Specific categories of types of hydrothermal alteration were mapped, including jasperoid, decarbonatization of carbonate host rock, dolomitization, and argillic alteration. Surface mapping of mineralization was limited to indigenous limonite, including both disseminated indigenous limonite after pyrite and gossan (Figure 9).

The most conspicuous alteration products in the map area are jasperoid replacement bodies. The competent nature of this replacement silica is responsible for the high relief of Lookout Mountain and Ratto Ridge. Three levels of replacement have been denoted on the map, from incipient to strong they are: fracture-controlled, breccia, and complete replacement (Figure 9). The map units that host jasperoid in the map area include the Cambrian Eldorado Dolomite, Cambrian Hamburg Dolomite, Ordovician Pogonip Group, and the Devonian Sentinel Mountain/Bay State Dolomite.

Decarbonatization accompanies most carbonate rocks in the map area, and is defined by the removal of carbonate material, and manifests itself in outcrop as bulk and local rock volume-loss, destruction of original rock texture, bleaching, and increased porosity (vugs, pock-marks, etc.). This mode of hydrothermal alteration rarely forms outcrops and typically forms recessive areas. Therefore, this alteration was mostly observed in road cuts and the walls of the Lookout Mountain open-pit mine. Decarbonatization and to a lesser degree jasperoid formation, are the alteration types most closely tied to formation of Carlin-type ore.

Limonite minerals identified during mapping included goethite, hematite, and local jarosite. The distribution of limonite was mapped by strength (incipient to strong), and abundance (low to high), and was further characterized as being either fracture controlled, disseminated, and/or pervasive. Where limonite was abundant, pervasive, and strong the term “gossan” was used, as these relatively competent, massive, vuggy siliceous limonitic bodies were easily distinguishable and well exposed (Blanchard, 1968). They likely represent weathered zones of massive sulfide. Altered igneous outcrops commonly exhibited “pin-head” indigenous limonite, suggestive of weathered disseminated pyrite. In contrast, random fractures stained with goethite and hematite are likely exotic limonite and do not indicate the fractures were once coated with sulfides, but, rather, suggest weathering of nearby sulfides.

Argillic alteration was mapped only in igneous rocks where feldspars or other silicates were completely replaced by clay, and was dominantly recognized in local igneous bodies which

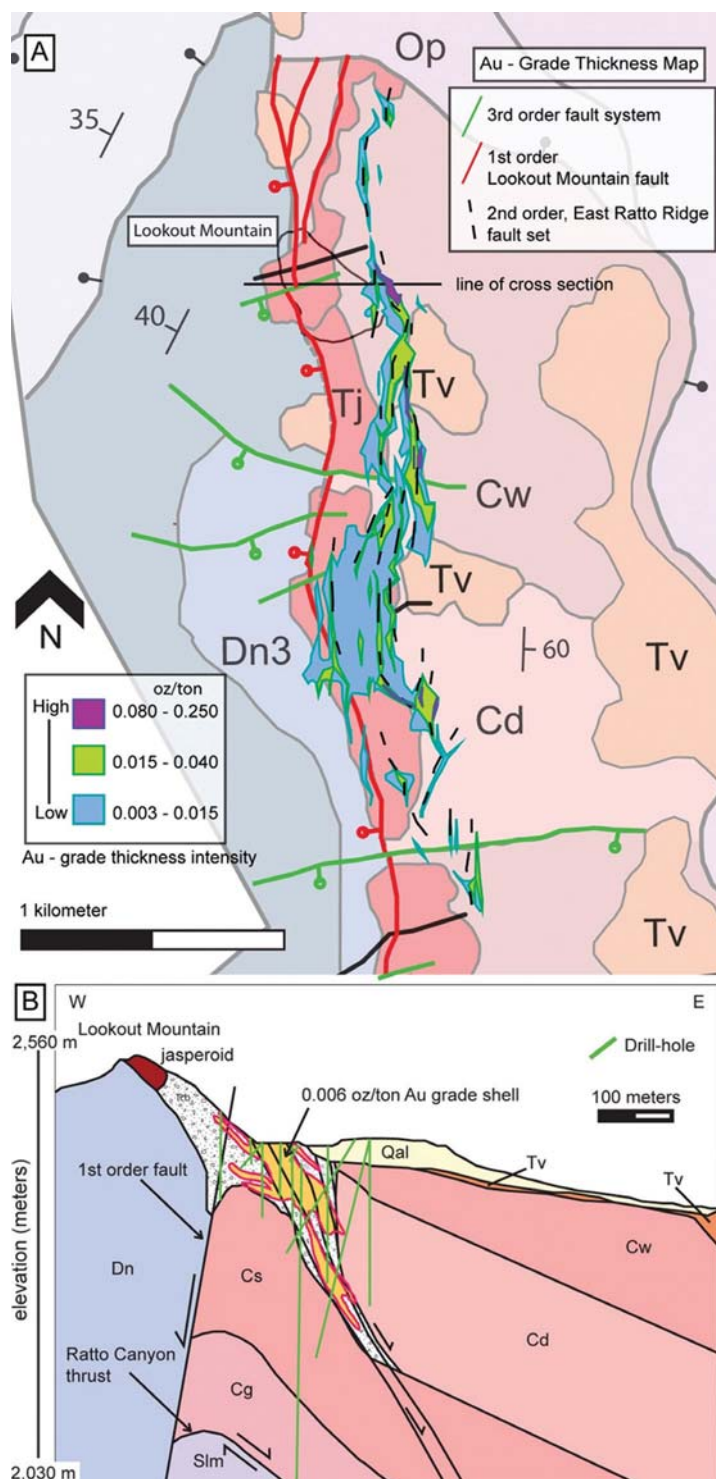


Figure 8. (A) Au grade-thickness map of Lookout Mountain. Dashed traces of individual, down-to-the-east faults of the 2nd-order, East Ratto Ridge fault system are shown. The following technique was followed for construction of the gold grade thickness map: A grade thickness calculation is as follows: for each assay interval the gold grade was multiplied by the thickness (in feet) of the interval (thickness = interval top minus the interval bottom), thus giving the grade-thickness for the interval. For the individual drill-hole, the sum all grade-thickness intervals were given a cutoff value (TRC's cutoff was 0.005 ounces gold per ton). There are two methods for plotting the location of the summed GT value. First is by collar coordinate, which works well for vertical holes, but not for angle holes, especially if the assay interval is at significant depth. For an angle hole the coordinate value for the midpoint of the summed grade-thickness zone (true thickness) and interval values is calculated and then projected onto the 2D plane, where other grade-thickness values are located. The midpoint was the average of the easting and northing values of all samples above the cutoff grade. Data supplied by TRC. (B) Cross section (drafted by TRC) showing geometry of Au mineralization at depth, and illustrating the system of 2nd- order East Ratto Ridge fault system.

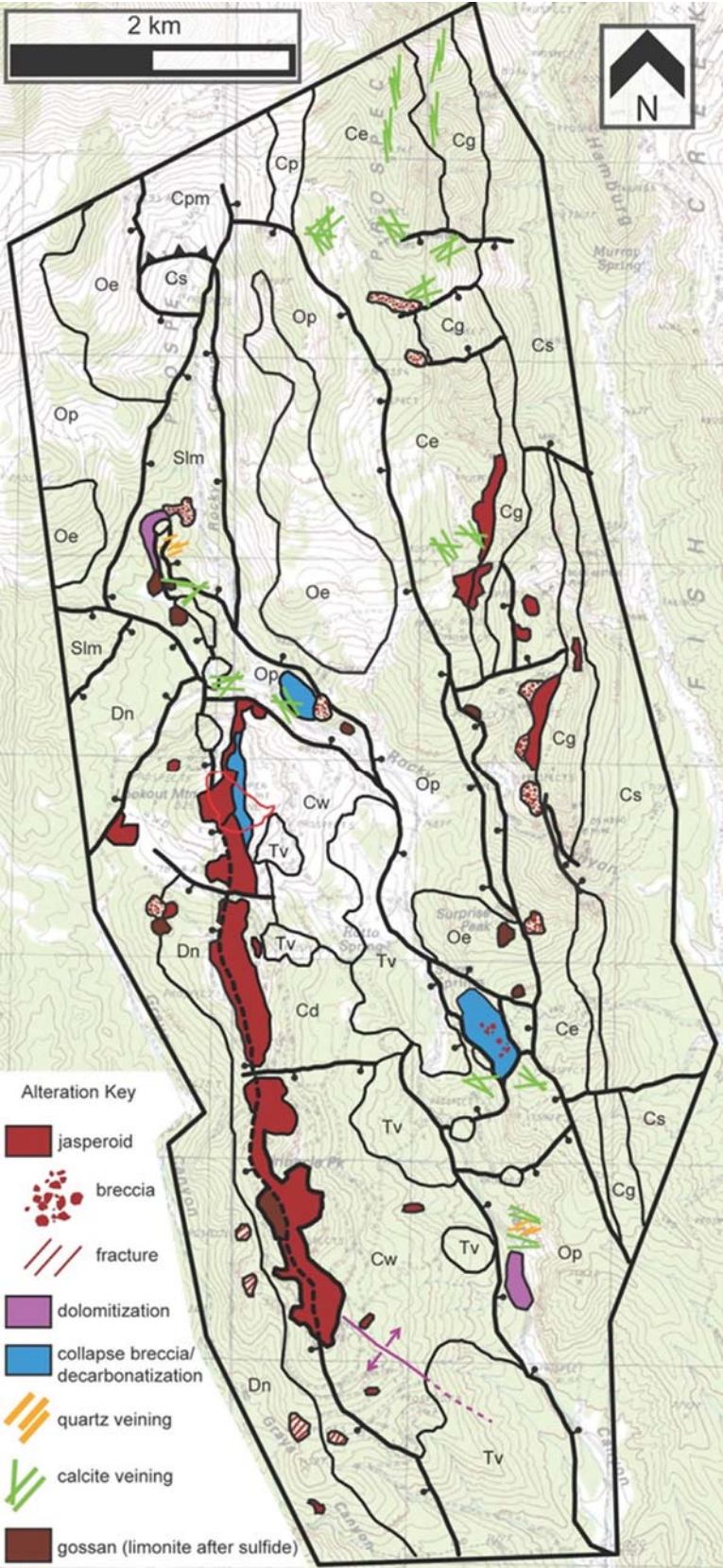


Figure 9. Alteration map, simplified from Di Fiori et al. (2014). Lithologic fill colors are removed for clarity. Argillic alteration omitted because of scale. Guide to map symbols shown in Figure 4.

contained feldspar phenocrysts. Since most igneous bodies are dikes emplaced along faults and/or fractures, argillic alteration is interpreted to demarcate hydrothermal fluid pathways along these zones. However, in some cases we could not rule out argillization of plagioclase by weathering. Argillic alteration was also observed in the Cambrian Dunderberg Shale.

Carlin-type gold deposits in the map area

Carlin-type gold mineralization in the map area is hosted primarily within the Cambrian Hamburg Dolomite and Dunderberg Shale, as well as within the Cambrian Eldorado Dolomite and Ordovician Pogonip Group carbonates. Beginning in the late 1970s these disseminated gold deposits, coincident with north-northwest trending, ridge-forming jasperoid bodies, were targeted for development and exploration. Lookout Mountain was mined from 1987 to 1988, producing 17,700 ounces of gold (Long et al., 2014A). TRC is currently seeking to develop and expand resources in the area. The current measured and indicated resource is 508,000 ounces of gold in 28,940,000 tons at an average grade of 0.018 ounce per ton (oxidized material) (Timberline Resources, Corporation, 2013).

Jasperoid formation, silicification, decarbonatization, and argillization in the subsurface are widespread within and adjacent to zones of Carlin-type mineralization, and extend the entire length of Ratto Ridge (Steininger et al., 1987; Timberline Resources Corporation, 2013). Along Lookout Mountain and Ratto Ridge, disseminated gold is hosted primarily within the Cambrian Hamburg Dolomite and in the overlying the Cambrian Dunderberg Shale. Alteration in the subsurface consists of collapse breccias in the Hamburg Dolomite which are wide near the surface, but narrow down dip along 2nd-order, east-dipping faults. Gold mineralization also occurs in jasperoid bodies that top Ratto Ridge, up to depths of 1,500 feet, and is associated with strongly anomalous concentrations of arsenic, mercury, and antimony anomalies (Long et al., 2014A).

In addition to the deposits along Ratto Ridge and Lookout Mountain, other areas within the project boundaries have alteration and geochemical characteristics consistent with Carlin-type gold mineralization. Directly east of Lookout Mountain, the Oswego Mine area displays decarbonatization of the host rock (vuggy texture and destruction of rock texture), as well as varying stages of jasperoid formation (fracture controlled to complete replacement). Anomalous mercury, antimony, and arsenic have also been recorded in past drilling endeavors (Timberline Resources, Corporation, 2013). Alteration and geochemistry consistent with Carlin-type mineralization is also found north to northeast of Lookout Mountain within the Ordovician Pogonip Group further east in the Oswego structural trend, where the Cambrian Eldorado Dolomite serves as the primary host rock.

Gold mineralization occurs along the trace of the Lookout Mountain fault and its footwall, where it expands eastward toward Ratto Canyon (Figure 8A-B). Gold mineralization is

spatially coincident with the northwest, north, and northeast-striking, 2nd-order antithetic faults within the footwall of the Lookout Mountain fault (the East Ratto Ridge fault system). Rupturing of the 2nd-order fault system instigated hydrothermal fluid flow and interaction with host rocks, specifically dissolution and silicification of carbonate to form jasperoid in the Hamburg Dolomite, and replacement of carbonate and illite by quartz and kaolinite in the Dunderberg Shale. Active faulting and water rock interaction was perpetuated by volume loss and formation of collapse breccia that resulted from carbonate dissolution. Petrographic work indicates water-rock reaction was accompanied by pyrite and realgar. Scanning electron microscopy and energy dispersive spectroscopy of ore samples indicates hydrothermal alteration was accompanied by deposition arsenian pyrite, commonly on rims of diagenetic pyrite, and later realgar (Long et al., 2014A).

DISCUSSION

Structural evolution of the map area

The Early Cretaceous construction of the Eureka culmination, a ~20 km-wide, 80 km-long anticline (Long et al., 2014B), generated the underpinning structural architecture, and set the stage for later extension (Figure 10A). The map area occupies the approximate hinge zone of this regional-scale culmination. The culmination is interpreted by Long et al. (2014A) as a fault-bend fold that was constructed by motion on the east-vergent, blind Ratto Canyon thrust over a Cambrian to Silurian footwall ramp at depth (Figure 10A).

After construction of the Eureka culmination, motion on 1st- and 2nd-order normal faults took place (Figure 10B), and is interpreted as the result of gravitational collapse of this regional structural high. This faulting can be bracketed between Late Cretaceous (ca. 86 Ma), the age of contact metamorphism in northern Rocky Canyon that is cut by the Dugout Tunnel fault, and late Eocene (ca. 37 Ma), based on the overlapping relationship of the sub-volcanic unconformity across 1st- and 2nd-order faults (Long et al., 2014B). Because of a similar strike, steeply west-dipping geometry, and amount of throw, the Lookout Mountain and Dugout Tunnel faults are interpreted to have been active at similar times. The Dugout Tunnel fault maintains ~3 km offset throughout the map area. The Lookout Mountain fault maintains ~2.5 km of offset through the southern half of the map area, and abruptly decreases in offset north of Lookout Mountain. Toward the north, this offset is distributed among 2nd-order structures of the Rocky Canyon fault system (Figures 4, 5B, 7, 10B), which is interpreted to be coeval with the Lookout Mountain Dugout Tunnel fault systems.

An additional set of east-dipping, antithetic, 2nd-order faults, the East Ratto Ridge fault system, is present within the footwall of the Lookout Mountain fault (Figures 8A-B and 10B). This fault set is characterized by steep (~50–70°) dips and proximal spatial relationships with highly-thinned Cambrian

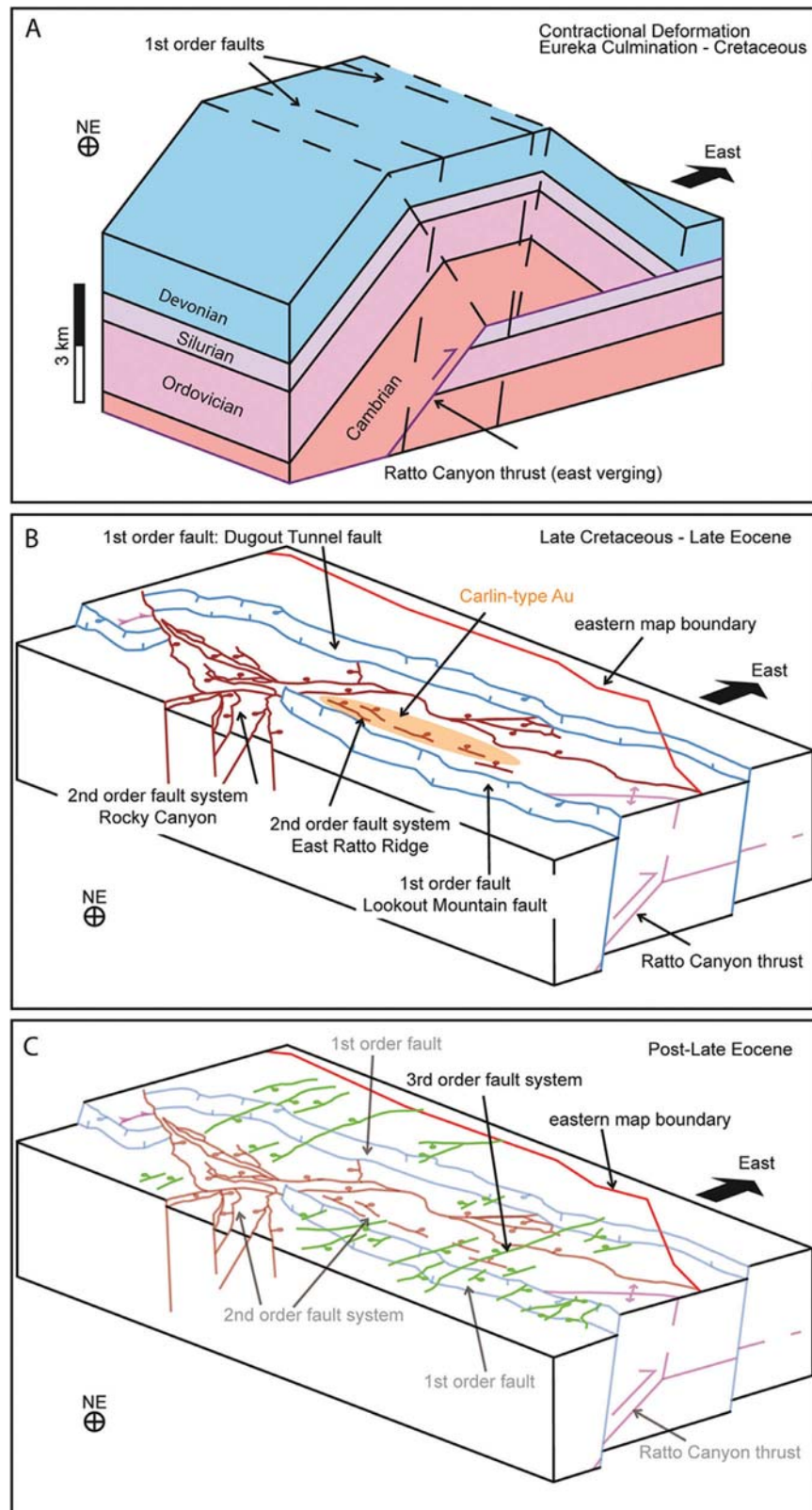


Figure 10. Block diagrams showing the temporal evolution of structural geometry and mineralization of the map area. (A) Late Cretaceous construction of Eureka culmination. Thick dashed lines represent future traces of the 1st-order Lookout Mountain and Dugout Tunnel faults. (B) Late Cretaceous to late Eocene motion on 1st-(blue) and 2nd-order (red) extensional structures. Location of Carlin-type deposit (gold) is shown. (C) Post-late Eocene formation of set of 3rd-order normal faults (green).

Hamburg Dolomite that underwent significant decarbonatization (Figures 6B and 8B). Due to their amount of offset (100s of meters) and geometry relative to the Lookout Mountain fault, these faults are interpreted to be coeval with the 1st - and 2nd -order fault systems as well.

Finally, the 3rd- order system of east-northeast striking, small-offset normal faults were the last to deform the map area, as they cut 1st- and 2nd -order extensional structures (Figure 5B, 8A, and 10C). Offsets of jasperoid bodies indicate post-late Eocene motion on these faults.

Spatial patterns and structural controls on Carlin-type mineralization

Based on the stratigraphic level of the late Eocene unconformity across the Lookout Mountain fault, Dugout Tunnel fault, Oswego fault, and East Ratto Ridge fault system, and the presence of rhyolitic dikes of presumably late Eocene age that intrude along Lookout Mountain fault and Rocky Canyon fault system, motion on these structures had to have been completed by the late Eocene, and therefore preceded Carlin-type mineralization.

In an attempt to assess structural controls on the spatial patterns of mineralization, a gold grade-thickness map (Figure 8A) was generated from data obtained from TRC drill holes along Lookout Mountain and South Lookout Mountain, where all mineralization was assumed to be of Carlin-type origin and late Eocene age. Additionally, TRC's cross sections drawn perpendicular to the mineralized trend (e.g., Figure 8B) were used to examine structural controls at depth and whether they were consistent with in the interpreted fault controls mapped on the surface.

In the map area, zones of elevated grade thickness trend sub-parallel to the strike of the Lookout Mountain fault, with the majority of the zones confined to the footwall (Figure 8A-B). The zones of moderate grade thickness (green polygons) have a distinct linear geometry, which trends sub-parallel to the Lookout Mountain fault. This pattern mimics the map pattern of structures of the East Ratto Ridge fault system. The close

proximity from one fault to another allowed for increased permeability due to generation of interconnected networks of damage zones (Caine et al., 1996). These 2nd-order faults are interpreted to have been integral for creating zones of localized fluid flow and thus, were favorable sites for mineralization. The majority of the mineralization related to the Lookout Mountain fault is spatially coincident with, and was strongly controlled by, this 2nd -order antithetic fault system.

Testing predictions for mineralization in accommodation zones

An accommodation zone is defined as an area of faulting and/or folding that transfers slip between larger structures (Faulds and Varga, 1998). These zones manifest themselves as belts of overlapping fault terminations and can separate systems of either synthetic or antithetic faults (Faulds and Varga, 1998). The majority of the map area occupies such an accommodation zone (Figure 4, 5B, and 10B); the 1st -order Lookout Mountain and Dugout Tunnel faults are interpreted to be genetically linked, and due to style of deformation, respective geometries, and spatial distribution of offset, and the 2nd-order Rocky Canyon fault system is interpreted to represent an accommodation zone that connects them (Figure 11A). Specifically, this accommodation zone represents a synthetically-breached relay ramp, using the classification scheme of Faulds and Varga (1998).

Wall-damage and linking-damage zone structures are proposed to control the migration of fluids and influence the localization of gold mineralization within accommodation zones (Figure 11B) (Micklethwaite, 2011). A damage zone is defined as the volume of deformed wall rocks around a fault surface that results from the propagation, initiation, and the build-up of slip along faults. Damage zones are classified into different geometric types depending on their location relative to the master faults in an accommodation zone (Kim et al., 2004). They are categorized as tip-damage zones, linking-damage zones (e.g., stepovers), and wall-damage zones, which represent faulting and fracturing in the proximal wall-rock region of a fault. Under this terminology, we interpret that the East Ratto Ridge fault system represents a wall-damage zone that formed in the footwall of the Lookout Mountain fault. The location of this wall-

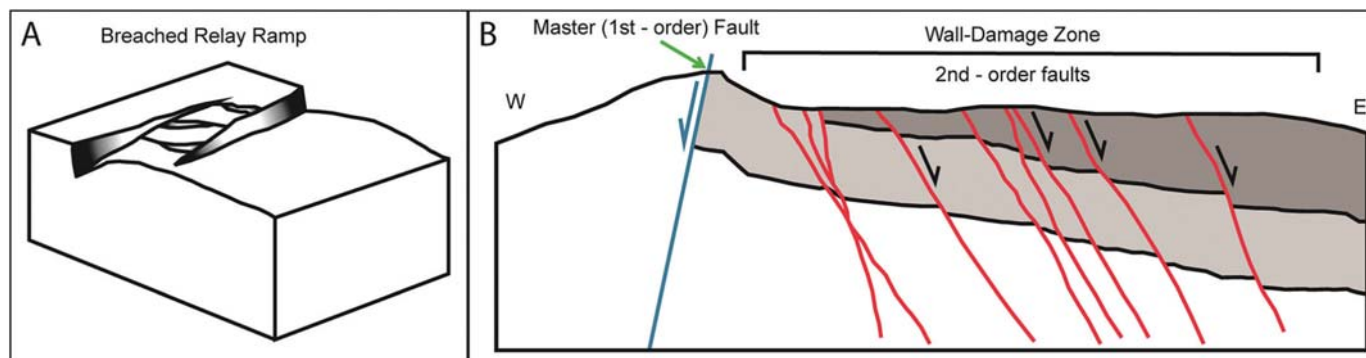


Figure 11. A) Schematic breached (faulted) relay ramp accommodation zone; modified from Faulds and Varga (1998). B) Schematic diagram of a wall-damage zone of a master (1st-order) fault (blue) and a series of antithetic, 2nd-order faults (red); modified from Micklethwaite (2011).

damage zone relative to the proximal Ratto Canyon relay ramp to the north is due to its position near the northward terminus of the Lookout Mountain fault. The eastward dip of the East Ratto Ridge fault system, which is antithetic to the master Lookout Mountain fault, is likely due to the structures taking advantage of the eastward dip of bedding. Here, the East Ratto Ridge fault system is interpreted to be a wall-damage zone proximal to a master structure of a faulted relay ramp. This structural environment was fundamental for the requisite ground preparation for the formation of the Carlin-type ore-deposit.

CONCLUSIONS

1. The Early Cretaceous construction of the Eureka culmination generated the underpinning structural architecture for subsequent extension, which was accommodated by coeval 1st- and 2nd-order normal fault systems, between ca. 86 and 37 Ma. A 2nd-order normal fault system transfers displacement between the 1st-order faults. Finally, a 3rd-order normal fault set crosscuts all earlier structures, and is presumably post-late Eocene.
2. The timing of Carlin-type mineralization in the footwall of the Lookout Mountain fault is interpreted to be late Eocene, synchronous with the emplacement of intrusive rocks along Lookout Mountain-Ratto Ridge, proximal to mineralized zones. The majority of mineralization is spatially coincident with structures of the 2nd-order, antithetic East Ratto Ridge fault system, which are interpreted to either pre-date or be contemporaneous with the fluid flow responsible for the formation of the Carlin-type ore body.
3. Wall-damage zone structures are proposed to control the migration of fluids and influence the localization of gold mineralization in accommodation zones. The 2nd-order East Ratto Ridge fault system, which is antithetic to and in the immediate footwall of the 1st-order Lookout Mountain fault, is interpreted to represent a wall-damage zone. Therefore, mineralization patterns in the south Eureka district confirm predictions for structural controls on mineralization in accommodation zones.
4. The southern Eureka mining district exhibits several ideal structural conditions for Carlin-type gold mineralization. These include: 1) major pre-ore normal fault systems that served as first-order conduits for hydrothermal fluids, and 2) an accommodation zone developed between the first-order faults, in which zones of dense fault intersections and wall-damage fault zones focused upwelling hydrothermal fluids, water-rock interaction, dissolution, silicification, and sulfidation of carbonate-bearing rocks, and deposition of gold. The southern Eureka mining district serves as an excellent example of a favorable structural setting for Carlin-type gold mineralization, which can be applied as a predictive structural framework in exploration elsewhere.

REFERENCES CITED

- Armstrong, R.L., 1968, Sevier orogenic belt in Nevada and Utah: Geological Society of America Bulletin, v. 79, p. 429–458.
- Best, M.G., Barr, D.L., Christiansen, E.H., Gromme, S., Deino, A.L., and Tingey, D.G., 2009, The Great Basin Altiplano during the middle Cenozoic ignimbrite flareup: insights from volcanic rocks: International Geology Review, v. 51, p. 589–633.
- Blanchard, R., 1968, Interpretation of leached outcrops. Nevada Bureau of Mines and Geology. Bulletin 66 (196 pp).
- Caine, J., Evans, J., and Forster, C., 1996, Fault zone architecture and permeability structure: Geology, p. 1025–1028.
- Dahlstrom, C.D.A., 1969, Balanced cross sections: Canadian Journal of Earth Sciences, v. 6, p. 743–757.
- DeCelles, P.G., and Coogan, J.C., 2006, Regional structure and kinematic history of the Sevier fold-and-thrust belt, central Utah: Geological Society of America Bulletin, v. 118, p. 841–864.
- Dickinson, W.R., 2002, The Basin and Range Province as a composite extensional domain: International Geology Review, v. 44, p. 1–38.
- Di Fiori, R.V., Long, S.P., Muntean, J.L., and Edmondo, G.P., 2014, Preliminary geologic and alteration maps of Lookout Mountain, Ratto Ridge, and Rocky Canyon, southern Eureka mining district, Eureka, Nevada. N Nevada Bureau of Mines and Geology Open-File Report, scale 1:10,000.
- Faulds, J. E., and Varga, R. J., 1998, The role of accommodation zones and transfer zones in the regional segmentation of extended terranes, *in* Faulds, J. E., and Stewart, J. H., eds., Accommodation zones and transfer zones: Regional segmentation of the Basin and Range province: Geological Society of America Special Paper 323, p. 1–45.
- Faulds, J., and Hinz, N., 2011, Assessment of favorable structural settings of geothermal systems in the Great Basin, Western USA: Geothermal . . . , v. 35.
- Henry, C.D., 2008, Ash-flow tuffs and paleovalleys in northeastern Nevada: Implications for Eocene paleogeography and extension in the Sevier hinterland, northern Great Basin: Geosphere, v. 4, p. 1, doi: 10.1130/GES00122.1.
- Kim, Y.-S., Peacock, D.C., and Sanderson, D.J., 2004, Fault damage zones: Journal of Structural Geology, v. 26, p. 503–517.
- Long, S.P., 2012, Magnitudes and spatial patterns of erosional exhumation in the Sevier hinterland, eastern Nevada and western Utah, USA: Insights from a Paleogene paleogeologic map: Geosphere, v. 8, p. 881–901.
- Long, S.P., Henry, C.D., Muntean, J.L., Edmondo, G.P., and Thomas, R.D., 2014A, Geologic map of the southern part of the Eureka mining district, and surrounding areas of the Fish Creek Range, Mountain Boy Range, and Diamond Mountains, Eureka and White Pine Counties, Nevada: Nevada Bureau of Mines and Geology Map 183, 1:24,000-scale, 2 plates, 36 p.
- Long, S.P., Henry, C.D., Muntean, J.L., Edmondo, G.P., and Cassel, E.J., 2014B, Early Cretaceous construction of a structural culmination, Eureka, Nevada, U.S.A.: implications for out-of-sequence deformation in the Sevier hinterland: Geosphere.
- Micklethwaite, S., Sheldon, H.A. and Baker, T., 2010, Active fault and shear processes and their implications for mineral deposit formation and discovery: Journal of Structural Geology, v. 32, p. 151–165.
- Micklethwaite, S., 2011, Fault-induced damage controlling the formation of Carlin-type ore deposits, *in* Steininger, R. and Pennell, B., eds., Geological Society of Nevada 2010 Symposium: Great Basin Evolution and Metallogeny, May 14–22, Sparks, Nevada: Geological Society of Nevada, p. 711–721.
- Nolan, T.B., 1962, The Eureka Mining District, Nevada: U.S. Geological Survey Professional Paper 406, p. 78.

- Nolan, T.B., Merriam, C.W., and Blake, M.C., Jr., 1974, Geologic map of the Pinto Summit quadrangle, Eureka and White Pine counties, Nevada: U.S. Geological Survey Miscellaneous Investigations Series, Map I-793: 1:31,680-scale, 14 p., 2 plates.
- Oldow, J.S., 1984, Evolution of a late Mesozoic back-arc fold and thrust belt, northwestern Great Basin, U.S.A.: *Tectonophysics*, v. 102, p. 245–274.
- Peters, S.G., 2004, Syn-deformational features of Carlin-type Au deposits: *Journal of Structural Geology*, v.26, p.1007–1023.
- Speed, R. C., and Sleep, N. H., 1982, Antler orogeny and foreland basin: A model: *Geological Society of America Bulletin*, v. 93, p. 815–828.
- Steininger, R.C., Klessig, P.J., Young, T.H., 1987, Geology of the Ratto Canyon gold deposits, Eureka County, Nevada, *in* Johnson, J.L., ed., *Bulk Mineable Precious Metal Deposits of the Western United States*, Guidebook for Field Trips: Geological Society of Nevada, Reno, p. 293–304.
- Stewart, J.H., and Poole, F.G., 1974, Lower Paleozoic and uppermost Precambrian Cordilleran miogeocline, Great Basin, Western United States, *in* Dickinson, W.R., ed., *Tectonics and Sedimentation: Society of Economic Paleontologists and Mineralogists Special Publication 22*, p.1306–28–57.
- Suppe, J., 1983, Geometry and kinematics of fault-bend folding: *American Journal of Science*, v. 283, p. 684–721.
- Taylor, W.J., Bartley, J.M., Fryxell, J.E., Schmitt, J., and Vandervoort, D.S., 1993, Mesozoic Central Nevada thrust belt, *in* Lahren, M.M., Trexler, J.H., and Spinosa, C., eds., *Crustal Evolution of the Great Basin and the Sierra Nevada: Geological Society of America Cordilleran/Rocky Mountain Sections Field Trip Guidebook*: Boulder, p. 57–96.
- Taylor, W.J., Bartley, J.M., Martin, M.W, Geissman, J.W., Walker, J.D., Armstrong, P.A., and Fryxell, J.E., 2000, Relations between hinterland and foreland shortening: Sevier orogeny, central North American Cordillera: *Tectonics*, v. 19, no. 6, p. 1124–1143.
- Timberline Resources, Corporation, 2013, Updated Technical Report on the Lookout Mountain Project, Eureka County, Nevada, USA.
- Wyld, S.J., 2002, Structural evolution of a Mesozoic backarc fold-and-thrust belt in the U.S. Cordillera: New evidence from northern Nevada: *Geological Society of America Bulletin*, v.114, p. 1452–1468.